Institutul de Chimie Macromoleculară "Petru Poni"
Iași, România

Interdisciplinary approaches for the analysis and protection of cultural heritage items

Abordări interdisciplinare în caracterizarea și protejarea unor obiecte de patrimoniu

Coordonator ştiinţific
Acad. Bogdan C. Simionescu

Doctorand
Oancea Andrei-Victor

Iași, 2020

Academia Română
Institutul de Chimie Macromoleculară „Petru Poni" din Iași

Nr. 6348/5.X.2020

Doamnei/Domnului.....

Vă facem cunoscut faptul că, în ziua de **29 octombrie 2020**, **ora 11:00**, în biblioteca Institutului de Chimie Macromoleculară „Petru Poni" din Iași, va avea loc susținerea publică a tezei de doctorat intitulată **„Abordări interdisciplinare în caracterizarea și protejarea unor obiecte de patrimoniu"**, **"Interdisciplinary approaches for the analysis and protection of cultural heritage items"** elaborată de chimist **Andrei-Victor Oancea**, în vederea conferirii titlului științific de doctor.

Comisia de doctorat are următoarea componență:

PREȘEDINTE: **Dr. Valeria Harabagiu**, Cercetător științific gradul I
Director al Institutului de Chimie Macromoleculară „Petru Poni" din Iași

CONDUCĂTOR ȘTIINȚIFIC: **Acad. Bogdan C. Simionescu**, Cercetător științific gradul I
Institutul de Chimie Macromoleculară „Petru Poni" din Iași

REFERENȚI: **Prof. Dr. Dana Ortansa Dorohoi**,
Universitatea "Alexandru Ioan Cuza" din Iaşi

Dr. Arheol. Cornelia-Magda Lazarovici, Cercetător științific gradul I
Institutul de Arheologie din Iaşi

Prof. Dr. Mircea Nicolae Palamaru,
Universitatea "Alexandru Ioan Cuza" din Iaşi

În conformitate cu Regulamentul privind organizarea și desfășurarea doctoratului pentru acordarea titlurilor științifice în Academia Română, vă trimitem rezumatul tezei de doctorat, cu rugămintea de a ne comunica în scris aprecierile și observațiile dumneavoastră.

Cu această ocazie, vă invităm să participați la susținerea publică a tezei de doctorat.

DIRECTOR,
Dr. **Valeria Harabagiu**

ACADEMIA ROMÂNĂ INSTITUTUL DE CHIMIE MACROMOLECULARĂ "PETRU PONI" IAȘI

Dezvoltarea temelor de cercetare studiate în cadrul acestei teze de doctorat nu a fost posibilă fără contribuţia şi îndrumarea unor cercetători care mi-au oferit posibilitatea de a aborda un subiect care îmbină, într-un mod armonios, ştiinţa şi frumosul.

Îi mulţumesc pe această cale conducatorul ştiinţific al lucrarii ***domnului Acad. Bogdan C. Simionescu****, care mi-a oferit posibilitatea de a alege şi aborda un subiect atât de fascinant, patrimoniul cultural, în cadrul tezei de doctorat.*

Cercetarea efectuată pe perioada studiilor doctorale nu ar fi fost posibilă fără sprijinul ***dr. Mihaelei Olaru,*** *din ale cărei cunoştiinţe şi expertiză am avut mult de învăţat şi care, prin exemplul ei, mi-a arătat calităţile la care fiecare cercetător ar trebui să aspire.*

Aş vrea să îi mulţumesc, în acelaşi timp, lui ***dr. George Bodi*** *care mi-a dat şansa de a lucra cu obiecte de o mare importanţă culturală, fragmente de ceramică de Cucuteni.*

Doresc să mulţumesc şi colegilor mei de laborator, ***dr. Cristi Ursu, dr. George Rusu*** *şi* ***ing. Corneliu Coţofană,*** *care m-au sprijinit în activităţile mele de cercetare.*

Multumesc colegilor din institut cu care am avut onoarea de a colabora.

Mulţumiri comisiei pentru amabilitatea de a evalua conţinutul ştiinţific al tezei de doctorat.

Mulţumiri Academiei Române pentru suportul financiar pe perioada parcurgerii stagiului de doctorat.

Table of contents

Introduction

Cultural heritage is the expression and embodiment of the ways of living specific to a community and passed on through successive generations and that includes practices, customs, places, values, objects and artistic expressions. Tangible Cultural Heritage consists of the extensive works created by humankind that includes places of habitation, cities, town, villages, structures, buildings, art works, documents, handicrafts, furniture, clothing, musical instruments, jewelry, religious, funerary and ritual objects, tools, equipment and industrial systems and machinery.

Paintings are two-dimensional representations of either real or imaginary objects, places, people or abstract ideas that are created by the application of paint on a flat surface. As their composition involves multiple materials, paintings are susceptible to degradation from multiple factors including light, temperature, humidity, air pollutants, mechanical shock and the growth of growth of bacteria, algae, fungus and other microorganisms. Ceramic artifacts of cultural and historical importance are clay and silica based objects molded in a certain shape and afterwards fired to high temperatures. While chemically very stable, ceramics do encounter degradation mostly due to mechanical shock, the breakdown of metastable phases formed during firing, the presence of soluble salts and the crystallization of water upon freezing. The analysis of paintings and ceramics is very difficult due to very heterogeneous nature of these items and, thus, requires complex measurements. Generally, the application of a single spectroscopic method is not enough and a combination of multiple techniques is required in order to elucidate the various structural and compositional aspects of an artifact.

When talking about artifacts and museum objects, one does not only mention objects with great spiritual, cultural and historic value but also of objects that have existed for hundreds if not thousands of years and curators and conservators would like to extend their life as much as possible. This comes in direct contradiction with normal commercial products used for the repairing and mending various objects because the timeframe for their service life is ephemeral in comparison. For this reason, when talking about conservation materials, conservationists do not talk about a product, but rather a treatment [70] which follows a cycle encompassing the application, the ageing and the removal of compounds that should not lead to any changes to the protected object. The research into conservation materials for ceramics is quite scarce [75,76] and many of the studies on ceramics only follow the

investigation of a number of properties and do not try to analyze the chemistry that rules the interactions between the conservation treatment and the protected ceramics. Only when the preservation of specific items of significant cultural importance was considered, such as Portuguese azulehos and heritage Chinese ceramics were more in-depth studies undertaken [80,82,83].

Both locally and within the Moldavian region there are a number of significant sites and museums of European and world interest, such as the Moldova National Muzeum Complex and the University Museum in Iași, the Cucuteni History and Archeology Museum and the Cucuteni Neolithic Art Museum in Piatra Neamț that house items of great importance for Romanian cultural heritage. Among the most important and wide-known Romanian cultural heritage artifacts are Cucuteni pottery, which impress both in terms of production quality and distinctive design. The unique shapes of decorations and characteristic way that abstracts motifs are represented have fascinated both archaeologists and the world at large and offer clues about how the prehistoric people understood the universe around them. The Moldova National Museum Complex also houses masterpieces by Romanian and foreign artists, some which are an integral part of the Romanian treasury. Among the most important artworks featured in the collection of the museum are paintings by two of the most influential Romanian artists, Nicolae Grigorescu and Ștefan Luchian. The authors contributed greatly to the development of Romanian painting both though the style and the themes they approached and contributed to the creation of the Romanian identity and culture as a whole. The study of Cucuteni pottery and of the paintings of Nicolae Grigorescu and Ștefan Luchian would be a great addition to the current knowledge of Romanian cultural heritage.

The current thesis, “Interdisciplinary approaches for the analysis and protection of cultural heritage items” is divided into 6 chapters that includes an introductory and an original research section. The thesis is 170 pages long and contains 47 figures, 14 tables and 225 references.

Chapter 1 presents important concepts regarding cultural heritage, details the structure, importance and degradation phenomena that affect paintings and ceramics, lists the most important analysis techniques employed in the study of ceramics and paintings and the most recent studies on the topic, introduces the requirements for conservation materials and summarizes the most important articles on conservation materials for ceramic artifacts. Chapter 2 details the scope and objectives of the thesis and highlights the relevance of the current study for expanding the knowledge of Romanian

cultural heritage. Chapter 3 presents the analysis of Cucuteni pottery from the archaeological site of Hoisești – la pod and details a multi-analytical investigation that includes both the study of the likely raw materials and of the prehistoric ceramics by means of SEM-EDS, XRD, FTIR, micro-Raman and optical microscopy, and discusses various aspects of the production technology employed by the specialized craftsmen. Chapter 4 details the analysis of paintings by Nicolae Grigorescu and Ștefan Luchian and includes investigations performed on micro-samples, ATR, SEM-EDS, XPS and micro-Raman, and portable non-invasive measurements, Raman, XRF and NIR. The study is focused both on the pigments and materials used by the two masters and the evolution of the techniques over the course of time and the current state of degradation that affects the works of art. Chapter 5 presents the synthesis of a new nanostructured material, AMF, and the evaluation of its protection efficiency in comparison to the widely used Paraloid B-72 (PB-72). The chapter focuses on the changes that occur to the structure of the two materials both in bulk, by means of FTIR, and on the surface level, by nano-FTIR, over the course of ageing showing the role of AMF as a chemically active coating and highlighting the role of the nano-FTIR technique. At the same time, the colour variation imparted to the ceramic substrate and the evolution of the contact angle are discussed. Chapter 6 lists the conclusions of the current thesis, highlighting the most important aspects derived from this original research.

The current summary presents the main results of the original research detailed in chapters 3, 4 and 5 and respects the names and numbering of the chapters, figures, tables and references.

ORIGINAL RESEARCH

CHAPTER 3. Analysis of ceramic artifacts – the study of Hoisești pottery

3.3. Characterization of raw materials

Initial granulometric analysis of soil samples collected from the perimeter of the Cucuteni settlement revealed that they belong to either the low or medium clay category. To determine if local raw materials were used in the production of the pottery, 4 samples collected from the slope created by the watercourse were subjected to structural analysis. The 4 soil samples were collected at various depths and included alluvial soil with a greyish hue with various degrees of pigmentation.

The XRD diffractograms of the raw clays (Fig. 1) revealed that they have a similar mineral composition, the only differences being the percent amount of each mineral phase [117]. The identified minerals are: quartz, micas including illite/muscovite and biotite, K-feldspar, plagioclase, kaolinite, dolomite and calcite. The results of the Rietveld refinement showed that samples 2 and 3, most likely raw clays used for pottery production have an average calcium oxide concentration of 7 %, indicating that the raw materials fit into the calcareous clay category.

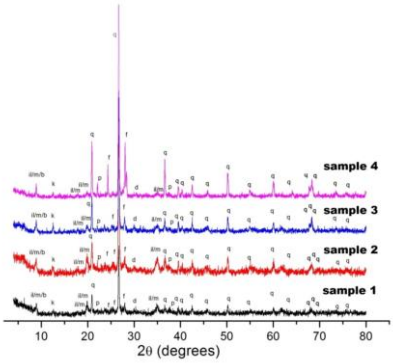

Figure 1. X-ray diffractograms of glycolated raw clay samples: b – biotite, d – dolomite, f – feldspars, k – kaolinite, il/m – illite/muscovite, p – plagioclase, q – quartz [117].

Due to the low Raman scattering of most clay minerals, the only silicate minerals encountered in the micro-Raman spectra were quartz and albite alongside calcite and metal oxides such as the TiO_2 polymorphs anatase and rutile and the MnO_2 pyrolusite. The FTIR analysis relied on second order derivative spectra and identified minerals include: illite/muscovite, quartz, biotite, kaolinite, dolomite, calcite, chlorite, talc, montmorillonite, albite, orthoclase, anatase, rutile, hydroxyapatite and pyrolusite.

3.4. Characterization of Hoisești pottery samples

Over the course of the analysis, 9 samples from Hoisesti-la pod were investigated, 3 belonging to each type of pottery, coarse, semifine and fine. The categories were established based on the density of the matrix and the number and size of inclusions, with fine ceramics presenting the most dense matrix, with the lowest number of inclusions, while coarse ceramics had the largest number of pores and largest and highest number of inclusions.

The SEM-EDS (Fig. 5) analysis investigated the morphology of the ceramic paste and the composition of individual features. It was able to show that all samples presented extensive vitrification which, in the case of ceramics based on calcite rich raw materials, develops at temperatures of over 850° C. At the same time, individual particles of metal oxides and different types of minerals, such as feldspar and micas, were observed. Salt depositions and bacteria associated with the degradation phenomena were also encountered. In the case of sample 73, particles with the specific morphology of volcanic ash of smooth facets with bubbles protruding the surface were found.

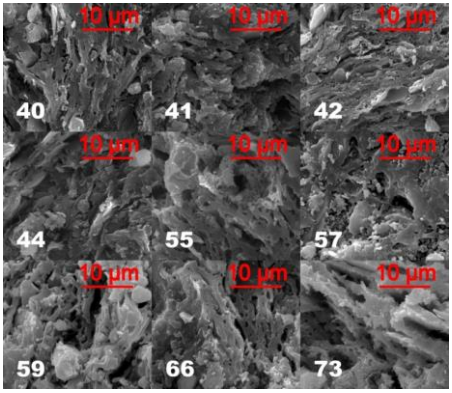

Figure 5. SEM images illustrating the morphology of the ceramic fabric. The numbers in the bottom left corner of each image indicate the sample. Samples 40, 66 and 73 are coarse, 41, 42 and 44 are semifine and 55, 57 and 59 are fine ceramics [117].

The XRD analysis of the ceramic shards revealed a similar mineralogical composition of the samples, with the exception of sample 73 (Fig. 7). In regard to silicate and alumino-silicate minerals, quartz, K-feldspar, the wollastonite pyroxenoidinosilicate, plagioclase and the diopside clinopyroxene were encountered in all samples. While present in all other samples, illite/muscovite was noticeably absent in sample 57, while olivines were encountered only in sample 73. As for the metal oxides, hematite was found in all the samples, magnetite in samples 40, 41, 42, 66, wüstite in samples 42, 55, anatase in samples 44, 59, rutile - in sample 44 and ilmenite in samples 55, 73. Sample 42 was the only one containing well crystallized calcite, according to the XRD measurements.

Quartz, illite/muscovite and plagioclase are the silicate mineral phases also encountered in the raw materials, while clinopyroxene, pyroxenoids as well as high temperature plagioclase are formed during the firing.

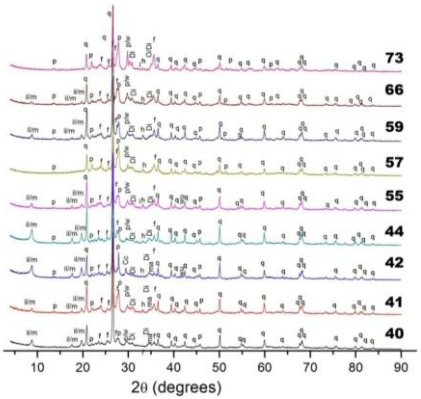

Figure 7. X-ray diffractograms of ceramic samples: Cc - calcite, Di - diopside, f - feldspars, i - ilmenite,il/m - illite/muscovite, h - hematite, ma - magnetite, O - olivines, p - plagioclase, Q - quartz, W - wollastonite, wu -wüstite.

The compounds identified during Raman analysis are as follows: quartz, anatase, rutile, pyrolusite, hematite, magnetite, amorphous carbon, wüstite, calcite, graphite, microcline, sanidine, hydroxyapatite, muscovite, ilmenite, clinoenstatite, porphyrin and animal fats. The second order derivative computations of the FTIR spectra allowed the identification of bands characteristic to the following compounds: pyrolusite, muscovite, wollastonite, orthoclase, rutile, anorthite, diopside, gehlenite, forsterite, fayalite, ilmenite, clinoenstatite, hydroxyapatite, hematite, magnetite, wüstite, anatase, quartz.

3.5. Production technology of Hoisești pottery

One of the most important aspects of pottery production is the firing temperature and determining it requires establishing the presence of the following mineral phases (i) the primary mineral phases which were present in the raw materials and that do not change during heating, (ii) the neo-formed crystalline phases which result during the high temperature chemical reactions of the various raw material components; (iii) secondary phases which refer to the high temperature amorphous phases that result upon firing.In the current study, the XRD analysis was able to determine the presence of the following high temperature minerals: pyroxenes including diopside and wollastonite, olivines such as forsterite and fayalite and plagioclase. Alongside these, the FTIR investigation were able to also identify the characteristic bands of anorthite, gehlenite, hydroxyapatite and clinoenstatite. The high temperature compounds and minerals observed in the Raman spectroscopy spectra included amorphous carbon, graphite, microcline, sanidine, and pyrolusite.

The main Si-O stretching band between 1100-1000 cm^{-1} is strongly influenced by the temperature reached during the firing of ceramic materials [140-142]. The increase in temperature elevates the band to higher wavenumbers due to the alteration of raw clays, the development of the amorphous phases and the formation of high temperature minerals. The Si-O band appears as a singlet in the 1084-1080 cm^{-1} interval in the case of samples 41, 55, 57 and 59, while for 66 and 73 it lowers to 1064-1059 cm^{-1}. In contrast, the stretching vibration appears as a doublet for samples 40, 42 and 44, with the two maxima being present at 1040-1039 cm^{-1} and at higher wavenumbers between 1080-1076 cm^{-1}. Based on these values, we can ascertain that samples 41, 55, 57 and 59 were fired at the highest temperatures of at least 900°C, while samples 66 and 73 were exposed to temperatures very close to 900°C. The lowest firing temperatures, between 800-900°C, were encountered for samples 40 and 42, 44.

The presence of plagioclase, wollastonite and diopside according to the FTIR and XRD measurements and the presence of extensive vitrification establishes that all the samples were exposed to temperatures in excess of 860°C. On the other hand, the absence of mullite in the XRD investigations indicates, however, that the firing did not reach temperatures higher than 950°C. While the mineral has been identified *via* optical microscopy at temperatures as low as 800°C [119], it appears in XRD measurements starting from 950°C [120]. The XRD Rietveld refinement showed that only three samples, 42, 44 and 40 contain lower amounts of quartz than the average value determined for the raw materials, implying that the mineral was intentionally used as temper in order to provide a higher resistance to the thermal shock. The likely source is the deepest layer from which raw clays were collected as it contains a much larger amount of quartz or perhaps another layer situated beneath it. The use of organic based temper such as fibres, straw, manure a.s.o. can only be suggested for the coarse ceramics as, upon firing, they lead to the formation of large pores which were not observable in the case of the fine and semifine shards with a dense matrix.

The results of the analyses are able to reveal that the craftsmen from the Cucuteni settlement of Hoiseşti had a good understanding of both the suitable raw materials required for the production of quality pottery that prevented the formation of defects during firing and the development of cracks, and of technological knowledge necessary for the firing process. The potters were, thus, able to reach high temperatures that were maintained in a narrow interval ranging from 860 to 950°C, which is characteristic of the use

of specialized kilns. The structural characterization of pottery revealed that the craftsmen of Hoisești had advanced technological knowledge and that locally available raw materials allowed for the production of good quality pottery, further reinforcing the conclusion that the settlement of Hoisești-La Pod is the first identified Cucuteni site specialized as a center of pottery production.

3.5. Exterior materials

The most striking feature of sample 73 is the use of volcanic ash as temper, clearly identified on the basis of the SEM images. This is most surprising, considering that the geology of the site of Hoisești - La Pod shows no presence of volcanic activity. This was the first encounter of volcanic ash being used as temper in the production of Cucuteni pottery. Its use of temper in antiquity is well known due to its good properties that allowed for the firing of ceramic wares at much higher temperatures than calcite. The use of volcanic ash in sample 73 is further reinforced by the identification of high temperature minerals associated with volcanic activity including clinoenstatite, fayalite and forsterite. As such, the distinct composition and morphology of the sample indicates that it was not locally produced and that actually it originated in another settlement. While at the time the production location of the fragment has not been determined, it is likely a distant location considering that the nearest geological features that contain volcanic ash are situated 60 km from the site of Hoisești.

Hematite and TiO_2 used for the decorations were found in low concentrations in the raw materials and the lack of sources, where they could be extracted at the archaeological site indicates that these too came from a different location and were transported with the aim to produce pottery.

The presence of material from outside sources at Hoisești - La Pod further reinforces the idea that trade connections had developed between different types of Cucuteni communities.

CHAPTER 4. Analysis of cultural heritage paintings – the study of masterpieces by Nicolae Grigorescu and Ștefan Luchian

4.3. Analysis of pigments and materials used by Nicolae Grigorescu

The current thesis focused on the identification and structural characterization of the pigments and materials used by Nicolae Grigorescu in three paintings, “Old Lady with Basket”, “The Young Shepherd” and “The

Return from Fair", which are part of the collection of the Art Museum of Iași, Romania.

The XRF investigations revealed that lead was the most abundant element in all analysis points, in both preparation areas with a white to grey hue, as well as in areas with various colours indicate that the artist used lead white, $2PbCO_3 \cdot Pb(OH)_2$, not only for the ground, but also for the development of the different color tones. White lead was widely used by impressionists like Grigorescu in the preparative layers due to its optical properties that allowed it to infer opacity to "body" color and, as such, greatly enhance the luminosity of other pigments. The pigment also improves the drying properties of paints which allowed for artworks developed in the "en plein air" method, important for impressionists, to be quickly completed. Analysis of "The Young Shepherd" showed the presence of low amounts of Zn, which suggest that Grigorescu did also use zinc white, ZnO, though only to a small extent. Other pigments identified by XRF included chrome yellow, strontium yellow, ochres, vermilion, red lead, red earths, mars colours and viridian. The SEM-EDS analysis of blue grains observed by optical microscopy showed high amounts of Si, S, Al and Na, characteristic to the sulfur rich alumino-silicate composition of ultramarine. At the same time, the morphology of the grains which presented sharp corners was indicative of natural ultramarine, as the artificial pigment generally has rounded features. Unlike XRF, the EDS analysis did identify As in the samples, characteristic of either orpiment or realgar.

XPS measurements detected sulfur only in the fragments collected from "Old Lady with Basket" and "The Return from Fair". The deconvolution of the signal curves (Fig. 13) indicated the presence of four types of groups (sulfate, sulfite, elemental sulfur and polysulfides) at roughly the same binding energies in both samples.

The presence of polysulfides, the chromophore responsible for the rich blue color of ultramarine indicate that Grigorescu did in fact use this pigment. While sulfate, sulfite and polysulfides are present, both in natural and artificial ultramarine native elemental sulfur are encountered only in lapis lazuli [157-159]. The identification of the S^0 in the analyzed samples indicates that Grigorescu, as opposed to most impressionists, used natural ultramarine.

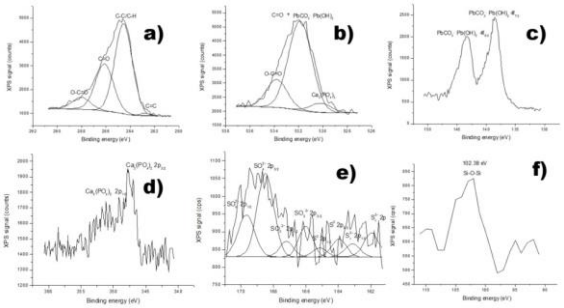

Figure 13. XPS narrow scan spectra of a) C 1s, b) O 1s, c) Pb 4f d) Ca 2p e) S 2p f) Si 2p regions for micro sample collected from "Old Lady with Basket" [144].

While FTIR and NIR were found to be useful in the identification of the linseed oil used for the binder and of the animal skin glue and calcite and gypsum used for the ground, in the case of the pigments they were somewhat limited and only allowed for the discrimination of associated minerals and materials.

4.4. Degradation processes in the paintings of Nicolae Grigorescu

Elemental analysis, XRF and EDS, revealed the presence of large amounts of S in the masterpieces related to the decay of pigments such as lead white, chrome yellow and vermilion due to sulfuration, which is a slow process that occurs in the presence of sun light and hydrogen sulfide [150,151,166-168]. In the case of lead white, the formation of the black lead sulfide, galena, is encountered in all studied paintings and is particularly evident in "Old Lady with Basket" [155]. The degradation process can also help explain the great variety of yellow hues that are encountered in the paintings, especially in the case of "Old Lady with Basket", with chrome yellow changing to darker shades, even brown, while lemon yellow going greenish in oil paints. FTIR measurements showed the formation of metal carboxylates which form upon the saponification reaction between the linseed oil and the metal cations in the pigments. While in the case of "Old Lady with Basket" and "The Young Shepherd" the intermediate esters and subsequent acids that form upon hydrolysis of the triglycerides from oils are still visible, they are completely gone in "The Return from Fair", indicating greater degradation.

In the case of the other techniques, the Raman measurements were able to highlight the degradation of white lead due to formation of new carbonate species $xPbCO_3 \bullet yPbS$ under the influence of H_2S from the surrounding atmosphere, while NIR investigations were helpful in ascertaining the alteration of linseed oil, with the formation of hydroperoxides and alcohols.

4.5. Analysis of pigments and materials used by Ștefan Luchian

The study of the technique and materials employed by Ștefan Luchian relied on the investigation of two representative paintings, namely "Chrysanthemums" and "Roses" from the "Moldova" National Museum Complex.

For the white pigments, EDS analysis found that Ba, Ca, Pb and Zn were present in all areas of interest indicating that Luchian used a combination of barium white, chalk, lead white and zinc white ZnO. Yellows shades, on the other hand, were created using cadmium yellow, strontium yellow, and ochres based on hematite and lepidocrocite. Purple grains observed by optical microscopy were found to contain cobalt purple based on cobalt phosphate, while red particles contained vermilion. In regard to green areas, while the presence of Cr allowed for the identification of viridian, the detection of Cu implied the use of either verdigris or copper resinate. Only two blue grains were observed under optical microscopy and the presence of significant amounts of Fe in both suggests that Luchian used Prussian blue.

The most significant discovery in the EDS analysis was the unexpected identification of indium in three distinct areas. Literature [150] does point to the possible use of indium oxide as a yellow pigment at the time when Luchian painted "Chrysanthemums". The large amounts of indium, over 20 %, in all three grains indicate that the metal cannot be associated with any impurity of the various materials used for the production of the painting and that it was intentionally applied, likely for its bright yellow color. In order to confirm the finding by another technique, the very laborious analysis of the grains by XPS was undertaken and in the analysis point carbon, indium and oxygen were detected. The broad bands of In $3d_{3/2}$ and $3d_{5/2}$ indicated the presence of multiple contributions which included the signal from both In_2O_3 and from In^0. The O 1s spectrum contained, along with the C-O-C and O-

C=O groups, a large contribution from the In_2O_3 grain [172].The distinct composition of the grain seems to be indicative of the production process involved in the manufacture of the pigment. The absence of any other elements except In, C and O suggests that $In(OH)_3$ was the likely precursor, while the presence of metallic indium suggests that a reduction reaction due to the photocatalytic activity of $In(OH)_3$ occurred. The other major contribution of the XPS technique to the current study involves the identification of Co in one of the analysis points as it is consistent with the cobalt-doped zinc oxide structure [176,177]. The production of both Rinmann's green and cobalt green involve the addition of minute quantities of cobalt to ZnO and their presence in areas with different colors due to their low tinting power would be consistent with the SEM/EDS and optical microscopy investigations.

The Raman technique was able to add a large number of pigments to the known number of pigments in the composition of Luchian's pallet. For the development of red hues, Luchian used both traditional materials such as ochres and vermilion, but also alizarin crimson and azoic pigments such as PR 57:1. All the white pigments identified by the EDS analysis, barium white, zinc white and lead white were also confirmed in the Raman measurements. Alongside chromate based yellows such as strontium yellow, the Raman measurements were able to also identify the use of massicot. Although the EDS investigations revealed that blue grains contained Prussian blue, the Raman measurements showed that for blues and purples Luchian also used ultramarine and cobalt purple. Darker pigments that were observed included carbon black and cassiterite, while in regard to binders and varnishes, the use of beeswax was identified.

The FTIR (Fig. 25) measurements were helpful in the analysis of organic components such as the proteinaceous binder used in the development of the ground layer, due to the characteristic amide I, amide II and amide III bands, and of the cellulose fibers in the canvas identified by the stretching vibrations of glucose chains. The analysis showed that the binder contained both beeswax and resins, which can be associated with the painting technique first employed by impressionists by which wax is used for the stabilization of paintings. The minerals identified in the FTIR studies include preparation layer components like kaolinite, chalk and gypsum and pigments including green earths, lead white, goethite and cobalt purple.

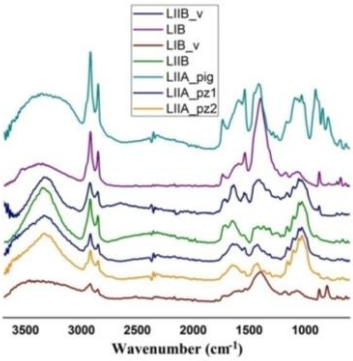

Figure 25. FTIR Spectra of samples from "Chrysanthemums": LIIB –microscopic sample, LIIB_v – microscopic sample with green hue, LIIA_pig – pigment area from canvas sample, LIIA_pz1 – canvas area from canvas sample, LIIA_pz2 - canvas area from canvas sample and "Roses": LIB – microscopic sample and LIB_v – microscopic sample with green hue.

The use of a large number of pigments in similar colors is a characteristic of Luchian, who embraced experimentation and relied on the contrast between the different hues to obtain specific optical effects. As such, the embrace of a large number of colors and his technique, which relied on the contrast between different hues, guided Luchian to use a wide array of pigments which ranged from traditional, such as lead white, vermilion, carbon black, to new or recently discovered at the time, such as azoic pigments (PR 57:1), to ones which, up to this point, were not previously documented in heritage paintings, indium yellow.

4.6. Degradation processes in the paintings of Ștefan Luchian

In the paintings of Luchian, the degradation of lead white, with the formation of sulfites and lead soaps, is the most widespread phenomenon being observed in both Raman and XPS measurements. While in the case of Raman spectroscopy, this is observable by the lack of no splitting of the ν1 Raman band indicating degradation due to the reaction with atmospheric H_2S, in the case of XPS spectroscopy we are able to observe the exact degradation products. The deconvolution of the signal curve revealed the presence of degradation products including PbO and/or $Pb(OH)_2$, PbS and $PbSO_4$.

The FTIR measurements revealed the presence of a large number of metal soaps associated with the degradation of the binder and the subsequent reactions that occur with the various metal cations. Zinc carboxylate was, by far, the most widespread degradation product as it was identified in all FTIR measurements. Copper, calcium, and cadmium based carboxylates were also encountered and their identification relied on the symmetric and asymmetric

stretching vibrations. Other metal salts that could be observed included oxalates, with Na and Ca being the most widespread, on account of the high reactivity of the two cations, while cadmium oxalate developed as a result of the degradation of cadmium yellow. The degradation of the binders and other organic materials was also highlighted by the presence of oxidation products including alcohols, carboxylic acids and hydroperoxides. The FTIR spectra were able to reveal the presence of the various stages of the degradation starting from early cleavage, with the formation of double bonds, to the advanced alteration, with the creation of aldehydes and acids.

4.7. Comparison of the painting methods of Nicolae Grigorescu and Ștefan Luchian

While clear contrasts between Grigorescu and Luchian can be observed starting from the preferred color and hues they use in their paintings, the differences continue to their choice of types of pigments. Grigorescu is very conservative in the materials he uses, going to extreme lengths to only employ traditional pigments and still using the very expensive natural ultramarine in an age where most other impressionists employ the newly discovered much cheaper synthetic alternative. Luchian, on the other hand, uses a high variety of red and yellow pigments, which is quite characteristic of post-impressionist painters, showing a great desire for experimentation. His use of varied novel and unique pigments is impressive, as he even employs very rare and previously unreported indium yellow in his “Chrysanthemums” masterpiece. Luchian does, however, still embrace some of the methods his predecessors utilized and the analysis of his paintings were able to show that the painter continued to employ beeswax in the stabilization of the paint surface, a technique pioneered by impressionists.

The optical effects that the two masters rely on in their artworks come from two different painting methods. While Grigorescu brings brightness to his paintings, many which are set in an exterior setting, and employs light colors and a lot of white, using the lead white pigment, Luchian in his still lifes relies on the contrast between the various colors to highlight differences.

CHAPTER 5. Novel treatment for the conservation of ceramic artifacts

Synthesis and application of conservation materials

A new polymeric nanostructured material containing silsesquioxane, methacrylate and fluorine units that present desirable properties for conservation treatments, called AMF, was synthesized. The synthesis of AMF aimed to develop a new chemically active coating with the capability to operate, *via* specific photochemical transformations that take place at the level of the coating-air interface that allows for the protection of ceramic artefacts. It relied on the hydrolysis and polycondensation reaction between equimolar amounts of 3-(trimethoxysilyl)propyl methacrylate (TMSPMA) and (3,3,3-trifluoropropyl) trimethoxysilane (TFPTMS) in acidic conditions, with dodecylamine as surfactant in isopropyl alcohol. The reaction was carried out at a temperature of 40°C, with mechanical stirring, for a period of two weeks until NMR measurements showed the complete hydrolysis of methoxy groups.

The protective capabilities of the novel AMF treatment was evaluated as compared to the widely used commercial product Paraloid B-72 (PB-72), which is a methylacrylate-ethylmethacrylate copolymer (PMA/PEMA) in a 30/70 weight percent ratio. The two polymers were applied on individual square pieces cut from the ceramic samples from Hoiești – la pod site previously analyzed. The application involved immersing the ceramic samples into 10 % solutions of the polymers for a period of 6 minutes until the formation of bubbles could no longer be observed. Thin films of PB-72 and AMF were developed by depositing 0.5 ml of the 10 % solutions on glass plates. While for PB-72 drying was possible in ambiental conditions, for AMF the samples had to be dried under vacuum for 60 days. The drying and storage conditions were identical for the ceramics and thin films.

Characterization of conservation materials

The ^{1}H-NMR spectrum of AMF (Fig. 26) allowed the identification of the different H atoms in the polymeric structure and can be assigned to the trifluoropropyl, propyl methacrylate and silanol groups. The presence of the silanol groups and the absence of the characteristic signal of methoxy groups indicate the complete hydrolysis of the starting reagents. When considering that the TMSPMA and TFPTMS precursors were added in equal stoichiometric amounts and that the integral ratio of the CH_3 to Si-OH signals is of 3:1.8, we can establish that the degree of condensation is of 70 %.

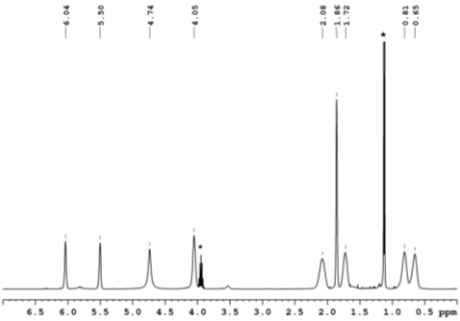

Figure 26. The ^{1}H-NMR spectrum of AMF, recorded in $CDCl_3$ at 400.1 MHz. The signals annotated with * are from isopropanol, the reaction solvent.

The ^{29}Si-NMR spectrum of AMF (Fig. 28) evidenced the presence of silanol units from constrained small cycles, linear and open chain groups, as well as cages and polycages. The ^{1}H and ^{13}C NMR spectra of PB-72 were consistent with those presented in reference literature and the signals can be attributed to the various PMA/PEMA groups.

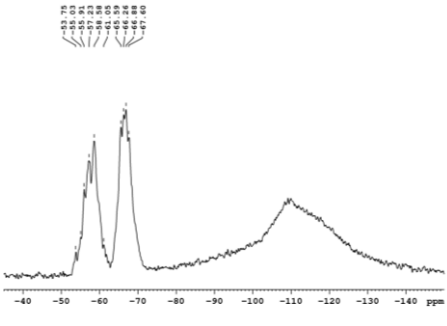

Figure 28. The ^{29}Si-NMR spectrum of AMF, recorded in $CDCl_3$ at 79.5 MHz.

In the FTIR spectrum of AMF (Fig. 36), the main Si-O-Si band is rather broad, indicating that the silsesquioxane network is mainly composed of randomly oriented components and not highly ordered structures. The siloxane bonds within the structure of AMF are arranged within small cycles, open cages associated to the ladder-like structures, cage-like and poly-cage structures. Among the different siloxane moieties, the absorption band assigned to cage-like structures present the highest intensity.

The FTIR spectrum evidenced the presence of the specific absorption bands of PB-72 (symmetric and asymmetric stretching vibrations of C-H group from the ester methyl, methylene groups and the methyl groups situated

in the α position to the main polymeric chain, CH deformation modes, free carbonyl stretching vibrations), as well as the presence of C=C double bonds. The presence of C=C double bonds before the ageing of the PB-72 thin film samples can be attributed to an incipient degradation process that occurred either during storage prior to deposition on the glass plates or to two days of exposure to ambinetal conditions during the drying of the thin films.

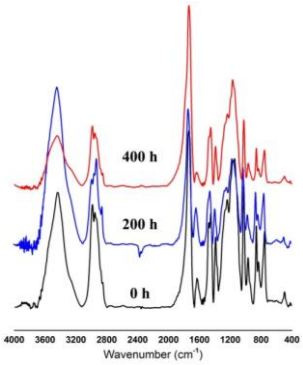

Figure 35. FTIR spectra of PB-72 thin film samples exposed to 0, 200 and 400 hours of UV ageing.

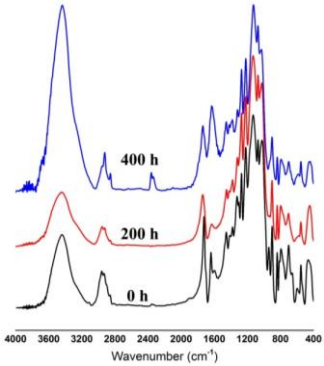

Figure 36. FTIR spectra of AMF thin film samples exposed to 0, 200 and 400 hours of UV ageing.

The Nano-FTIR analysis of the top layer of the AMF thin film (Fig. 38) revealed the presence of bands from silanol groups and silsesquioxane moieties based on small cycles, open cages and cage-like structures. The main carbonyl peak was shifted toward higher wavenumbers, most likely due to the preferential arrangement of the silsesquioxanes with the lowest crystallinity, to which the carbonyl groups are bound. Another major difference between the bulk and surface measurements is related to the intensity of the main carbonyl peak, which appears much weaker in the Nano-FTIR spectra. This behavior could be explained by the orientation of the CF_3 moieties towards the surface of the thin film, while the propyl groups migrate toward the interior of the sample causing the methylene units from the polymeric backbone to be arranged in a close-packed structure in the plane of the surface [211].

The Nano-FTIR spectrum of PB-72 (Fig. 37) is dominated by the strong absorption band of the PMA carbonyl stretching mode. The presence of carbonyl groups only from PMA fragments at the surface and the absence of any PEMA carbonyls can be attributed to the preferential orientation of these

groups with PMA migrating towards the surface, while PEMA tends to accumulate in the bulk. The Nano-FTIR investigations were also helpful in highlighting the incipient degradation process with the distinct signal of the C=C double bonds associated with the loss of side chain moieties appearing at 1646 cm^{-1}.

SEM investigations showed that the application of AMF on the ceramic samples did not lead to significant changes in surface morphology, thus indicating that the AMF coating is very fine and does not obstruct the pores of the substrate. In contrast, the PB-72 coating has the tendency to form a much thicker layer that, in many areas, completely covers the features of the underlying substrate.

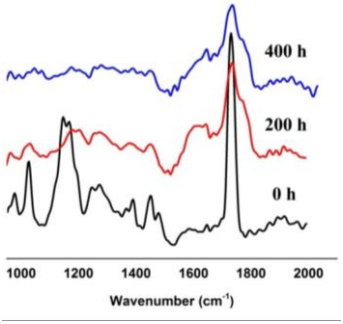

Figure 37. Nano-FTIR spectra of PB-72 thin film samples exposed to 0, 200 and 400 hours of UV ageing.

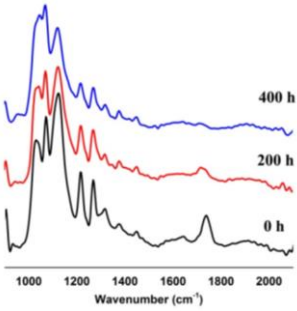

Figure 38. Nano-FTIR spectra of AMF thin film samples exposed to 0, 200 and 400 hours of UV ageing.

UV ageing of conservation materials

After the first UV ageing cycle, the FTIR measurements of AMF recorded a decrease for the intensity of OH peak (Fig. 36), which is usually associated with the photo-oxidation reactions to the hydroxyl groups that allow for the development of oxidation products with C=O chromophores in their structure [215]. The slight decrease of the bands in the fingerprint region and of the peak at 2986 cm^{-1} indicate the loss of volatile low molecular weight compounds due to UV degradation, though the phenomenon seems to be quite restricted. In the carbonyl region, the C=O stretching band registered both a lower intensity and a shift to higher wavenumbers, indicating the formation of production of degradation products, including aldehydes and/or esters.

After 400 h of UV exposure, the increase of the bands in the 2959-2854 cm^{-1} interval can be attributed to the photo-polymerization of the double bonds under the action of the UV light. While Si-O-Si stretching bands did not register significant changes, a minor decrease of the rest of the peaks could be observed, consistent with the loss of volatile small molecular weight compounds. At the same time, the increase and broadening of the C=O stretching band indicates a continued increase in the number of aldehyde and/or ester moieties.

In regard to PB-72, the most important changes observed by FTIR spectroscopy (Fig. 35) involve the -OH, CH, C=O and C-O-C groups. After the first ageing cycle, the bands of the OH region presented a great increase in intensity. While the bands in the fingerprint region do present a slight decrease, there is an obvious increase of the bands between 3000 - 2800 cm^{-1}, with the exception of the absorption peak at 2986 cm^{-1}. This behavior can be explained by the UV light induced photo-polymerization of the C=C double bonds that are formed on the surface layer [214]. Differences also appear in the carbonyl region, with the esteric C=O stretching band presenting an increase in intensity and broadening. At the same time, a small shoulder in the spectral region of the γ-lactones C=O stretching begins to appear [211,213]. The weak band of the C=C stretching vibrations increases, suggesting the formation of an ever increasing number of double bonds on the polymeric chain.

After the second ageing cycle, the FTIR spectra of PB-72 register a drop in the OH peak intensity which can be attributed to the photo-oxidation reactions that involve hydroxyl units that lead to the formation of oxidation products that contain C=O chromophores [215]. The increase of the bands from 2987 and 2955 cm^{-1} is likely due to the photo-polymerization of C=C double bonds, while the improvement of the bands in the 1500-990 cm^{-1} can be correlated with the formation of a large number of new types of oxidation products. In the carbonyl region, a distinct broadening and increase of the C=O stretching bands of esters and of γ-lactones can be observed. The peak of the C=C double bond, on the other hand, presents a significant decrease, indicating a drop in the number of the double bonds on the polymeric chain.

The evolution of the carbonyl functionality was evaluated by monitoring the value of the carbonyl index (C.I.), which is calculated by normalizing the C=O peak at 1723 cm^{-1} to bands that reference literature indicate do not present modifications due to UV ageing. While in the case of PB-72 the C=O peak was normalized to the stretching peak at 755 cm^{-1} of the

stable C-C bonds and the C.I. was calculated as A_{1723cm}^{-1}/ $A_{755\ cm}^{-1}$, for the AMF the stretching peak at 1269 cm^{-1} of the strong C-F bond was used and the C.I. was calculated as A_{1723cm}^{-1}/ $A_{1269\ cm}^{-1,}$ where A denominates peak absorbance. In regard to PB-72, the sharp increase of the C.I. (from 2.34 to 5.01) indicated the continuous development of C=O chromophores bearing oxidation products as a result of chain scission [215]. In regard to AMF, the constant decrease of the C.I. (from 1.86 to 0.87) indicates the C-O radicals formed due to C=O π bonds photo-destruction have a greater tendency to form crosslinked networks than undergo chain scission.

Only a slight decrease of the bands in the fingerprint region was observed in the nano-FTIR spectrum of AMF after the initial 200 h UV irradiation (Fig. 38). Lower intensities of the bands corresponding to cage-like, open-cages and small cycles were registered, while a new band at 1044 cm^{-1} could be observed, indicating the formation of a Si-O-Si network structure usually found in nano-SiO_2 films [216,217]. In the fingerprint region, a new band attributed to the CH in plane deformation vibration of >C=CH- groups indicates the formation of trisubstituted alkenes. In the carbonyl region, the main carbonyl band shows a sharp decrease, while a shoulder located at 1718 cm^{-1} appears, indicating the formation of saturated aliphatic ketones. At 400 hours of irradiation, the Si-O-Si asymmetric stretching of the nano-SiO_2 films increases in intensity and shifts to higher wavenumbers, at 1047 cm^{-1}, indicating a continued increase in the thickness of the film. Other changes to Si-O-Si bands include the increase of the intensity of the signals corresponding to small cycles and open cages (up to the initial intensity) and the continued decrease of the one related to cage-like structures. The main C=O stretching band almost disappears and the formation of carboxylic acids was observed.

The nano-FTIR spectrum of PB-72 showed the complete collapse of the bands in the fingerprint region after the first ageing cycle (Fig. 37). As follows, the decrease of the PMA carbonyl stretching (by more than half), as well as the development ofα, β-unsaturated γ-lactones, carboxylic acid dimers, trisubstituted alkenes and α,β-unsaturated esters were observed.

In regard to the sample exposed to UV light, for the full 400 h the nano-FTIR investigations revealed the perpetuation of the degradation process. The characteristic carbonyl stretching band continued to decrease, whilethecarbonyl doublet of the α, β-unsaturated γ-lactone increased. At the same time, new vinylene units and α,β-unsaturated esters are formed.

SEM investigations of the samples exposed to accelerated ageing show a clear degradation of the polymeric coating in the case of PB-72, with

the formation of micro-cracks, while no obvious differences could be observed for the AMF.

AFM images recorded for the unaged thin films of the polymeric coatings (Fig. 40) shows that both AMF and PB-72 create continuous smooth thin films. The initial UV ageing cycle does not cause significant changes for the AFM sample, with the general area of the thin film the coating is still smooth. The thin film is not damaged at 400 hours of UV irradiation, though the surface seems to be somewhat rougher likely due to the creation of segregated microphase domains and of the nano SiO_2 layer at the surface of the polymer.

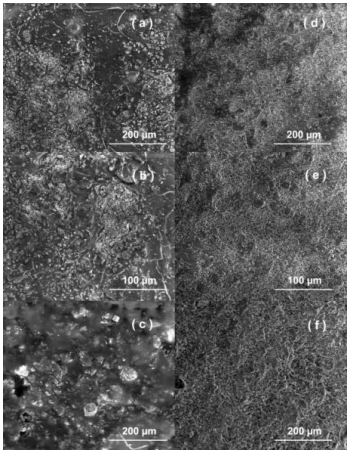

Figure 39. SEM images of samples 41 a), b) and 44 c) coated with PB-72 and of 41d), e) and 44 f) coated with AMF after 400 h of UV ageing showing the extensive damage due to crack formation observed in the case of the PB-72 coating.

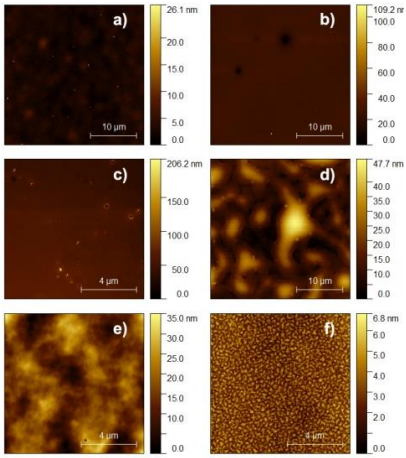

Figure 40. AFM images of thin film samples; a) unaged AMF thin film, b) unaged PB-72 thin film, c) AMF thin film exposed to 200h of UV ageing, d) PB-72 thin film exposed to 200h of UV ageing e) AMF thin film exposed to 400h of UV ageing, f) PB-72 thin film exposed to 400h of UV ageing.

As for the PB-72 samples, the situation is quite different and the advanced degradation of the polymer is clear. At 200 hours, the UV irradiation has caused flaking and cracking of the thin film layer, with large layers of the polymer peeling away from the surface of the sample. These defects allow

water and other degradation agents to penetrate deep within the substrate indicating that, at this stage, the coating no longer presents protective properties. After the second UV ageing cycle the situation is even more dramatic, with the large damaged sections sustaining further cracking and the whole polymeric surface appears as micrometer and nanometer sized fragments.

Colorimetric measurements were performed on both glass and ceramic substrates in order to establish the color changes that the two protective treatments undergo as a result of exposure to UV light and to determine how they influence the aspect of the coated ceramics. In regard to the AMF thin film sample, the initial UV light exposure cycle caused a photochemical aging confined to the top surface layer of the sample (slight decrease of ΔL*) and C=O moieties are generally involved in crosslinking reactions (decrease of Δa* and Δb*). The decrease of ΔE* suggests that AMF is able to absorb UV light and presents limited fading [221].

After 400 h of exposure to UV irradiation, a continuous decrease of ΔL* was noticed, indicating a darker surface. The increase of Δa* and Δb* shows that incipient degradation has started to affect the AMF polymer, however the small variations indicate that the phenomenon is very restricted. The continuous decrease of ΔE* seems to suggest that AMF presents a better protective effect as the irradiation time increases. The decrease of both ΔL* and ΔE* implies that only a minor degradation of AMF occurs, and the coating is able to remove many of the free radicals that result due to UV degradation and are responsible for the fading of the exterior surface.

The initial UV ageing cycle caused the PB-72 thin film to darken (decrease of ΔL*) accompanied by a greater degree of greenness (decrease of Δa*) and shift toward yellow (increase of Δb*). The color shift towards yellow observed in the PB-72 thin film is likely due to an increase in the concentration of C=O bearing chromophores due tochain scission [215]. The decrease of the Δa*, however, indicates that, while chain scission reactions lead to a greater number of C=O groups being created, they are consumed by crosslinking reactions. The increase of ΔE* and decrease of ΔL* suggests that the coating surface has partially faded areas due to polymeric chain scission. As a result, stress forms within the thin film causing the formation of cracks randomly oriented on the surface of the PB-72 coating responsible for whitening of the film and water penetration. The greater values of ΔE* and ΔL* after 400h of exposure to UV light reveals that the surface of the PB-72

thin film has faded completely as it is covered with large cracks also confirmed by SEM investigations.

The color variation inferred on the ceramic substrate by the two polymeric coatings does not follow the evolution observed for the thin film samples and various trends are observed among the different ceramic samples themselves due to the great inhomogeneity of the samples. Overall, however, the results clearly show that AMF has a better performance than PB-72 resulting in a lower color variation.

In order to properly establish the water repellant capabilities of both polymers, contact angle measurements were recorded for the thin films and the treated ceramic samples. Initial measurements recorded for the thin films deposited on glass revealed that both coatings are hydrophobic with similar values being recorded, 90° for PB-72 and 98.63° for AMF. The UV ageing resulted in only a slight reduction of the values of the contact angle for AMF (up to 82.13°), while for PB-72 a severe reduction of the contact angle (down to 18.3°) was observed.

As for the ceramic samples, both polymeric coatings presented different contact angle values as compared to the ones recorded for the glass substrate, which is consistent with the previous analysis which indicated a preferential orientation on the surface of certain groups. All ceramic samples coated with AMF presented higher contact angle values as compared to the ones recorded for the glass (up to 123.8°). In the case of PB-72, however, both lower and higher values were encountered. This behavior can be directly attributed to the different morphology and chemical composition of both polymers and substrates, as well as the high inhomogeneity and roughness of the ceramics.

After the initial UV exposure cycle, a sharp reduction in the values recorded for the contact angles of PB-72 coated ceramics was observed. All contact angle values decreased with over 50°, while in the case of the sample that presented the highest initial hydrophobicity, the drop is of almost 90°. This dramatic behavior of the PB-72 coated ceramics can be attributed to the formation of cracks within the polymeric layer. In the case of AMF, a completely different situation is encountered, where in 4 of the 7 coated ceramics a definite increase of the contact angle values was registered, up to 126.6°. This phenomenon is likely caused by the crosslinking reactions involving methacrylate groups that occur under the action of UV light and that result in the formation of novel hydrophobic $-CH_2-CH_2-$ moieties on the surface of the samples. The lower values that were observed are, however,

greater than the original values recorded for the samples coated with PB-72 and are likely due to the morphology and inhomogeneity of the ceramics.

At 400 h of UV exposure, the PB-72 coated samples present even lower contact angle values, indicating that the cracks present on the surface have begun to widen, allowing water to penetrate the polymeric layer and reach the substrate. In the case of AMF, an overall decrease of the contact angle values was also observed, though all values were greater than 90°.

Structural modifications of conservation treatments influenced by UV ageing

The modifications that appear in the structure of the two polymers during the UV ageing are intricately connected to the specific conditions they were submitted to. In this study, both the thin film and the polymeric coated ceramics were irradiated with a mercury lamp that emits light with a wavelength in the 200 to700 nm interval and kept in a 60 % humidity air atmosphere. As such, the samples were exposed to a large number of ozone molecules formed when the UV light with the wavelength lower than 242.4 nm interacted with oxygen molecules in the air atmosphere.

The main photodegradation phenomena of PB-72 observed after the first UV ageing cycle included chain scission of macromolecular chains followed by disproportionation, with the formation of C=C bonds. The FTIR and nano-FTIR analyses were able to identify the presence of α, β-unsaturated γ-lactones, α, β-unsaturated esters, vinylenes, trisubstituted alkenes and carboxylic acids under the form of dimers as the main degradation products. The degradation processes continued during the second ageing cycle, with extensive chain scissions of the polymeric chain being observed alongside the breakdown of the initial oxidation products. The different reactions involved in the UV ageing of PB-72 are presented in Figure 43. The PEMA fragments are much more stable and the main photodegradation phenomena that result in changes to their structure involve the macroradicals disproportionation, with the formation of double bonds that belong either to trisubstituted alkenes or to α, β-unsaturated esters. The carboxylic acid moieties observed in the FTIR and Nano-FTIR investigations likely form due to the oxidation of C=C double bonds in the presence of ozone (Fig. 44).

The degradation mechanism of AMF is similar, to a certain degree, to the one encountered for PB-72, and trisubstituted alkenes and α,β-unsaturated esters are formed (Fig. 45). Ozone can attack the C=C double bond resulting

inthe formation of ketones and aldehydes, which are further oxidized by H_2O_2 to carboxylic acid. The different behavior of the two compounds against UV photodegradation and the higher stability that was observed in the case of AMF can be attributed to the structure of the polymer.

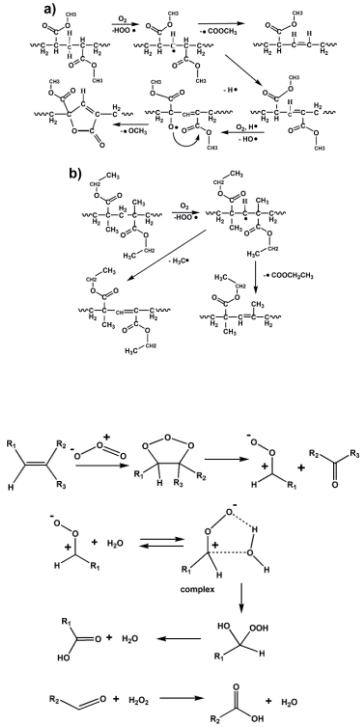

Figure 44. Ozonolysis reaction of C=C bonds.

Figure 43. Photo-oxidative degradation mechanism of PMA and PEMA segments present in the structure of PB-72.

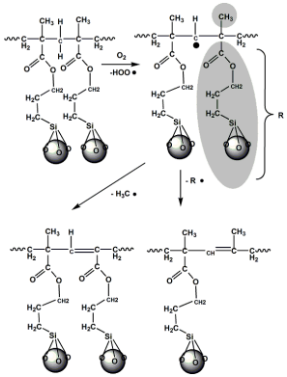

Figure 45. Photo-oxidative degradation pathway of AMF

The radiations with a wavelength lower than 253.7 nm are energetic enough to break the Si-O bond in silsesquioxane units. The conversion of silsesquioxane moieties into SiO_2 is controlled by the diffusion of ozone and atomic oxygen into the polymer [217]. After the first UV ageing cycle, the decrease of all Si-O-Si stretching bands characteristic to the silsesquioxane units in the nano-FTIR spectra indicates that all structures found on the surface are transformed into the SiO_2 network. After the second cycle of ageing, the only absorption band in the Si-O-Si region that continues to decrease is that of

cage-like structures, while the open cages and small cycles increased and returned to their original intensity. This implies that, aside from transforming into units of the SiO_2 type network, the cage-like structures also have the tendency to convert into more stable open cages and small cycles by reacting with the newly formed silanol and Si and O bearing radical species. The nano-SiO_2 network on the surface of the AMF material can act as a protective barrier at the interface between the polymeric surface and the surrounding atmosphere, providing additional functionality to the coating. At the same time, the recovery of ladder like structures after the second UV ageing cycle suggests that AMF presents "self-healing" capabilities.

While the energy dose was greater than the one required for the complete conversion of silsesquioxane units into a SiO_2 framework only a limited number of silsesquioxanes was altered. This behavior is likely due to fluorine and open-cage silsesquioxane units being present on the surface of the polymeric coating, which impeded the diffusion of ozone and atomic oxygen inside the AMF film. The re-organization of the top surface layer also likely resulted in fluoroalkyl side chains forming microphase-segregated domains that act like a physical barrier that provided greater water repellency properties and increased the UV ageing of resistance of AMF. The nano-SiO_2layer likely inhibited the formation of peroxidic species, the most important reactive species that are responsible in the fragmentation of the polymeric framework. In the current study the protective properties of the SiO_2 coating layer were also highlighted, especially considering the presence of terminal double bondsthatusually leads to decreased UV stability [225].

Salt mist accelerated ageing of ceramic samples

As opposed to UV ageing, the damage to the polymeric coating comes mainly from mechanical damage that results from the formation of salt crystals in the pores and cracks of the pottery that leads to flaking and cracking. This mechanical damage does not involve chemical modifications of the polymeric component, only the eventual removal of any soluble molecules. The damage inflicted by the salt mist is extensive and, during the course of the accelerated ageing in the case of two PB-72 coated samples, resulted in the complete detachment of portions from the outside layer of the ceramic.

After the salt mist cycles, significant weight loss was encountered in 7 of the 9 untreated pottery samples, highlighting the very destructive nature of these ageing tests. All samples displayed various degrees of powdering, but

only limited flaking. Four of the samples coated with PB-72 did not display significant degradation and their behavior can be correlated to the dense matrix resulting in increased toughness. Three other samples showed significant weight loss, but performed better that the untreated samples, with flaking and powdering being observed. The highest weight loss is observed in two samples where entire portions of the surface layer was removed as a result of the ageing test. Flaking seems to be the most prevalent behavior encountered in degradation and can be explained by the fact that grains are not detached individually from the ceramic matrix, but rather entire layers held together by the PB-72 are removed.

In regard to the AMF treatment, a very good evolution of the samples was observed, with only two samples showing weight loss and only in one case the value was greater than 0.1 %. The samples do not display any signs of flaking on the surface and only slight powdering was observed.

SEM investigations confirmed the extensive degradation encountered in the case of the PB-72 samples, showing both the flaking of the surface layer and the deposition of salt in exposed areas of the ceramic substrate.

CONCLUSIONS

The following conclusions can be drawn from the current study:

1. The multi-analytical archeometric study of Cucuteni pottery from the site of Hoisești – la pod revealed that the wares were fired in a restricted temperature interval indicating that local craftsmen were able to precisely control the firing process.
2. The potters had good technological knowledge about the production of ceramics and raw materials were locally available for the production of good quality wares.
3. The use of volcanic ash in the production of Cucuteni pottery was recorded for the first time in the Moldavian region.
4. The presence at Hoisești of ceramics of non-local provenance produced with volcanic ash (while the source is unkown, the nearest site with volcanic ash is 60 km away) shows that the settlement interacted with other communities and that trade connections were widespread and over large distances.
5. The investigation was able to corroborate other pedologic, geomorphologic, archaeologic and bio-archaeologic findings and indicated that the Hoisești-La Pod site was a specialized pottery production center.

6. The first in-depth studies into the composition of the pallet and the style of by Nicolae Grigorescu was performed showing that the artist used only a few pigments in his artworks.
7. Nicolae Grigorescu developed his colors using extensively lead white which he combined with a limited number of pigments.
8. For the first time the use of natural ultramarine was observed in the case of an impressionist painter at a time when the much more affordable artificial version was widely available.
9. The first ever identification of natural ultramarine in a work of art using the XPS technique was performed.
10. After more than 100 years after their creation the paintings of Nicolae Grigorescu are degraded with the formation of metal soaps being the most widespread degradation phenomenon.
11. The anlysis of the works by Ștefan Luchian showed that the painter had a very rich pallet which he used in his paintings in order to develop optical effects based on the contrasts between different hues.
12. The first ever identification of the use of indium oxide as a pigment in a cultural heritage painting was performed. While reference literature raise the possibility of the compound being employed as a shade of yellow its use has never been previously documented.
13. In the paintings of Luchian, the formation of zinc carboxylates and different types of oxalates is widespread due to the chemical reactions between the pigments and the aged binder.
14. The differences between the styles of the two painters, master and apprentice, that belong to consecutive art movement were highlighted with Grigorescu using only a few pigments and creating different colors with the addition of lead white and carbon black while Luchian had a rich pallet which he used to create specific contrasts.
15. The current reasearch highlighted the different problems associated with the analysis of cultural heritage and the need to use multiple analytical techniques and dedicated high performance equipment due to the complex structure, and inhomogeneous matrix of the artifacts for which only micro-sampling is generally desired.
16. A new polymeric nanostructured material containing silsesquioxane, methacrylate and fluorine units, called AMF, that can act as a chemically active coating was synthesized.
17. When compared to the widely used PB-72, AMF has a much better performance providing better water repellency and lower color variation.

18. UV and salt mist ageing tests were able to show that AMF is much more stable that PB-72.
19. Through the photochemical transformations from the coating-air interface, a nano-SiO_2 layer that provides improved protective properties is formed on the surface of AMF.
20. The structural modifications of AMF and PB-72 that occur over the course of UV ageing were analyzed and the mechanisms that govern the degradation processes were established.
21. The nano-FTIR technique is uniquelly suited for the analysis of surface phenomena such as the preferrential orientation of functional groups and the formation of degradation products.

The original research presented in the current thesis has been published in 2 articles in ISI indexed journals (cumulative impact factor 7.727), two other papers have been submitted for review and presented at 4 conferences (3 national, 1 international). A chapter accepted for publication by Elsevier details the state of the art on silsesquixane nanostructured materials for the protection of cultural heritage items.

Articles:

1. Oancea A.V., Bodi G., Nica V., Ursu L.E., Drobota M., Cotofana C., Vasiliu A.L., Simionescu B.C., Olaru M., Multi-analytical characterization of Cucuteni pottery, Journal of the European Ceramic Society, 37 (15), 2017, 5079-5098, https://doi.org/10.1016/j.jeurceramsoc.2017.07.018
2. Rusu R.D., Simionescu B., Oancea A.V., Geba M., Stratulat L., Salajan D., Ursu L.E., Popescu M.C., Dobromir M., Murariu M., Cotofana C., Olaru M., Analysis and structural characterization of pigments and materials used in Nicolae Grigorescu heritage paintings, Spectrochimica Acta Part A: Molecular and Biomolecular Spectroscopy, 168, 2016, 218-229, https://doi.org/10.1016/j.saa.2016.06.009

Book chapter:

1. M. Murariu, A. V. Oancea, C. Ursu, B. G. Rusu, C. Cotofana, B. Simionescu, M. Olaru, Surface properties of POSS nanocomposites, accepted to be published in Polyhedral Oligomeric Silsesquioxane (POSS) Polymer Nanocomposites book, Elsevier Publishing House

Communications:

1. Assessment of polymers as conservation treatments for ceramic fragments exposed to the action of UV radiations A. V. Oancea, G. Bodi, B.C. Simionescu, C. Coțofană, M. Olaru; A XXVII-a Sesiune de Comunicări Ştiinţifice a Institutului de Chimie Macromoleculară „Petru Poni" Iaşi, Progrese în ştiinţa compuşilor organici, Iași, 2-4 octombrie 2019
2. SEM-EDX pigment analysis of Stefan Luchian heritage paintings; M. Murariu, A. V. Oancea, M. Olaru; Conferința Facultății de Chimie, IasiChem 2018, 25-26.10.2018
3. Polymeric coatings for ceramic conservation; A. V. Oancea, M. Olaru; A XXVI-a Sesiune de Comunicări Ştiinţifice a Institutului de Chimie Macromoleculară „Petru Poni" Iaşi, Progrese în ştiinţa compuşilor organici, Iași, 5-6 octombrie 2017
4. Multi-pronged archaeometrical study of the Cucuteni A pottery from the site of Hoisești – La Pod; A. V. Oancea, M. Olaru, L. Ursu, M. Drobotă, C. Cotofana, G. Bodi; Die Cucuteni-Kultur und Ihre Südlichen Nachbarn Im 5. Jt. V. Chr., organizat de Academia Romana, Filiala Iasi in colaborare cu D.A.I. – Eurasien Abteilung, Iasi, 18-22 aprilie 2016

REFERENCES

[70] Horie C.V., Materials for Conservation: Organic consolidants, adhesives and coatings, Elsevier Science, 2010

[75] Constancio C., Franco L., Russo A., Anjinho C., Pires J., Vaz M.F., Carvalho A.P., J. Appl. Polym. Sci. 116, 2010, 2833–2839

[76] Zhao J., Luo H., Wang L., Li W., Zhou T., Rong B., Herit. Sci. 1, 2013, 12

[80] Costa D., Leal A.S., Mimoso J.M., Pereira S.R.M., MATERIALES DE CONSTRUCCIÓN, http://dx.doi.org/10.3989/mc.2017.09015

[82] Cultrone G., Madkourb F., J. Cult. Herit. 14, 2013, 304–310

[83] Zhao J., Li W., Luo H., Miao J., J. Cult. Herit. 11, 2010, 279–287

[117] Oancea A.V., Bodi G., Nica V., Ursu L.E., Drobota M., Cotofana C., Vasiliu A.L., Simionescu B.C., Olaru M., J. Eur. Ceram. Soc. 37 (15), 2017, 5079-5098

[119] Cultrone G., Rodríguez-Navarro C., Sebastián E., Cazalla O., de la Torre M.J., Eur. J. Mineral. 13, 2001, 621-634

[140] Shoval S., Optic. Mater. 24, 2003, 117-122

[141] Shoval S., Beck P., J. Therm. Anal. Calorim., 82, 2005, 609-616

[142] Shoval S., J. Therm. Anal. Calorim. 42, 1994, 175-185

[150] Eastaugh N., Walsh V., Chaplin T., Siddall R., Pigment Compendium.A Dictionary and Optical Microscopy of Historical Pigments, Elsevier, Oxford, 2008.

[151] Rebollo E., Nodari L., Russo U., Bertoncello R., Scardellato C., Romano F., Ratti F., Poletto L., J. Cult. Herit., 2013, 14 (3S), e153–e160
[152] Burgio L., Clark R.J.H., Theodoraki K., Spectrochim. Acta A Mol. Biomol. Spectrosc. 2003, 59, 2371–2389
[157] Tauson V.L., Goettlicher J., Sapozhnikov A.N., Mangold S., Lustenberg E.E., Eur. J. Mineral. 2012, 24, 133–152
[158] Tauson V.L., Sapozhnikov A.N., Shinkareva S.N., Lustenberg E.E., Geochem. Int. 2009, 47, 815–830
[159] Fleet M.E., Liu X., Harmer S.L., Nesbitt H.W., Can. Mineral. 2005, 43, 1589–1603
[166] Goltz D.M., Charleton K., Cloutis E., Grinberg P., Collins C., J. Analy. Atom. Spectrom. 2007, 22, 140–146
[167] Samain L., Gilbert B., Grandjean F., Long G.J., Strivay D., J. Anal. Atom. Spectrom. 2013, 28, 524–535
[168] Zanella L., Casadio F., Gray K.A., Warta R., Ma Q., GaillardJ.-F., J. Anal. Atom. Spectrometry 2011, 26, 1090–1097
[172] NIST X-ray Photoelectron Spectroscopy (XPS) Database
[176] Rasouli S., Moeen S. J., J. of Alloys Comps. 2011, 509, 1915-1919
[177] Gandhi V., Ganesan R., Syedahamed H.H.A.,Thaiyan M., J. Phys. Chem. C, 2014, 118, 9715-9725
[211] Zhang Y., Fan H., Wang Y., Zuo B., Zhang W., Wang S., Wang X., Soft Matter, 2015,11, 9168-9178
[213] Chiantore O., Trossarelli L., Lazzari M., Polymer, 2000, 41, 1657–1668
[214] Scherzer T., J. Polym. Sci. A Polym. Chem. 2004, 42, 894–901
[215] Shanti R., Hadi A.N., Salim Y.S., Chee S.Y., Ramesh S., Ramesh K., RSC Advances, 2017, 7, 112-120
[216] Kim Y., Zhao F., Mitsuishi M., Watanabe A., Miyashita T., JACS 2008, 130, 11848-11849
[217] Yamamoto S., Sonobe K., Miyashita T., Mitsuishi M., J. Mater. Chem. C, 2015, 3, 1286-1293
[221] Goiato M.C., Santos D.M., Haddad M F., Pesqueira A.A., Brazilian Oral Research, 2010, 24(1),114-9
[225] Sacchi B., Giannini L., Frediani M., Rosi L., Frediani P., J. Coat. Technol. Res. 2013, 10 (5), 649–657